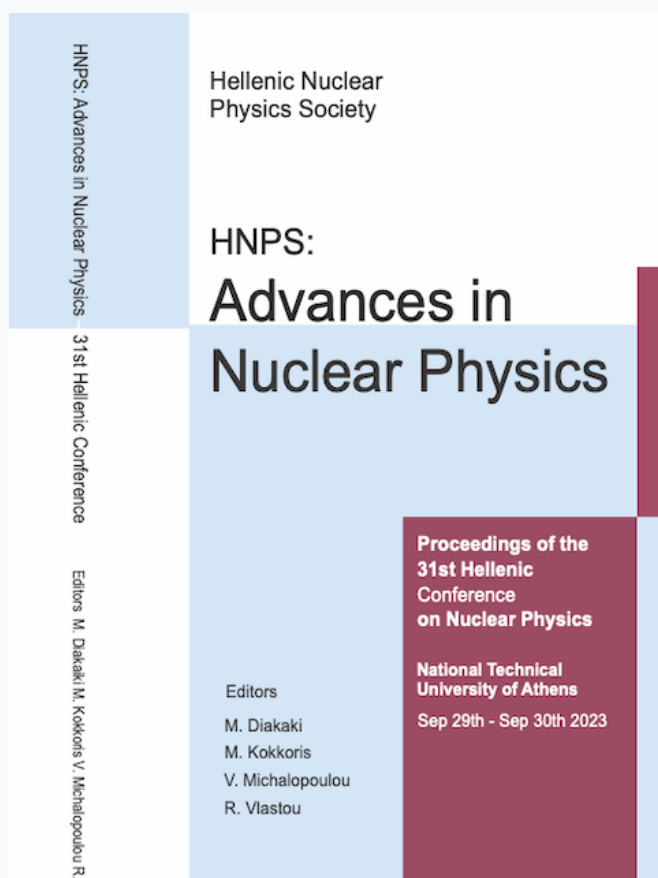


## HNPS Advances in Nuclear Physics

Vol 30 (2024)

HNPS2023



### Multinucleon Transfer Reactions in the $^{70}\text{Zn}$ (15 MeV/nucleon) + $^{64}\text{Ni}$ System: Detailed Studies of the Reaction Mechanism

*Stergios Koulouris, Georgios Souliotis, Francesco Cappuzzello, Diana Carbone, Athina Pakou, Clementina Agodi, Giuseppe Brischetto, Salvatore Calabrese, Manuela Cavallaro, Irene Ciraldo, Olga Fasoula, Jozef Klimo, Onoufrios Sgouros, Vasileios Soukeras, Alessandro Spatafora, Domenico Torresi, Martin Veselsky*

doi: [10.12681/hnpsanp.6245](https://doi.org/10.12681/hnpsanp.6245)

Copyright © 2024, Stergios Koulouris, Georgios Souliotis, Francesco Cappuzzello, Diana Carbone, Athina Pakou, Clementina Agodi, Giuseppe Brischetto, Salvatore Calabrese, Manuela Cavallaro, Irene Ciraldo, Olga Fasoula, Jozef Klimo, Onoufrios Sgouros, Vasileios Soukeras, Alessandro Spatafora, Domenico Torresi, Martin Veselsky



This work is licensed under a [Creative Commons Attribution-NonCommercial-NoDerivatives 4.0](https://creativecommons.org/licenses/by-nc-nd/4.0/).

### To cite this article:

Koulouris, S., Souliotis, G., Cappuzzello, F., Carbone, D., Pakou, A., Agodi, C., Brischetto, G., Calabrese, S., Cavallaro, M., Ciraldo, I., Fasoula, O., Klimo, J., Sgouros, O., Soukeras, V., Spatafora, A., Torresi, D., & Veselsky, M. (2024). Multinucleon Transfer Reactions in the  $^{70}\text{Zn}$  (15 MeV/nucleon) +  $^{64}\text{Ni}$  System: Detailed Studies of the Reaction Mechanism. *HNPS Advances in Nuclear Physics*, 30, 31–36. <https://doi.org/10.12681/hnpsanp.6245>



# Multinucleon Transfer Reactions in the $^{70}\text{Zn}$ (15 MeV/nucleon) + $^{64}\text{Ni}$ System: Detailed Studies of the Reaction Mechanism

S. Koulouris<sup>1,\*</sup>, G.A. Souliotis<sup>1</sup>, F. Cappuzzello<sup>2,3</sup>, D. Carbone<sup>3</sup>, A. Pakou<sup>4</sup>, C. Agodi<sup>3</sup>,  
G.A. Brischetto<sup>2,3</sup>, S. Calabrese<sup>3</sup>, M. Cavallaro<sup>3</sup>, I. Ciraldo<sup>2,3</sup>, O. Fasoula<sup>1</sup>, J. Klimo<sup>5</sup>,  
O. Sgouros<sup>3</sup>, V. Soukeras<sup>3</sup>, A. Spatafora<sup>2,3</sup>, D. Torresi<sup>3</sup>, M. Veselsky<sup>6</sup>

<sup>1</sup> Laboratory of Physical Chemistry, Department of Chemistry, National and Kapodistrian University of Athens, Athens, Greece

<sup>2</sup> Dipartimento di Fisica e Astronomia “Ettore Majorana”, Università di Catania, Italy

<sup>3</sup> Laboratori Nazionali del Sud, INFN, Catania, Italy

<sup>4</sup> Department of Physics and HINP, The University of Ioannina, Ioannina, Greece

<sup>5</sup> Institute of Physics, Slovak Academy of Sciences, Bratislava, Slovakia

<sup>6</sup> Institute of Experimental and Applied Physics, Czech Technical University, Prague, Czech Republic

**Abstract** The present work constitutes one of the few high-resolution mass spectrometric studies in the energy range of 15–25 MeV/nucleon in order to produce and identify neutron-rich projectile-like fragments from the reaction of  $^{70}\text{Zn}$  (15 MeV/nucleon) +  $^{64}\text{Ni}$ . We obtained high-quality experimental data from a recent experiment with the MAGNEX spectrometer at the INFN-LNS in Catania, Italy. The momentum distributions ( $p/A$ ), angular distributions and the production cross sections of various multinucleon transfer channels were studied thoroughly. Our experimental distributions shown in this contribution are compared with two dynamical models, the Deep-Inelastic Transfer (DIT) model and the Constrained Molecular Dynamics (CoMD) model. Subsequently, the code GEMINI is applied for the de-excitation of the primary fragments. The DIT model, designed to describe the sequential exchange of nucleons, yielded an overall fair description of the processes that correspond to nucleon exchange, but is not able to effectively describe parts of the distributions that refer to direct reaction mechanisms. The microscopic CoMD model calculations indicate that further optimization is needed, that is currently underway. The present work outlines an experimental approach to study peripheral reactions of medium-mass nuclei in the Fermi energy regime and an effort to pave a systematic way toward the efficient production of exotic neutron-rich nuclei.

**Keywords** Rare Isotope Production, Multinucleon Transfer, Magnetic Spectrometer, Particle Identification

## INTRODUCTION

Up to the present time, one of the main challenges of the nuclear community in rare isotope beam facilities around the world (see, e.g., [1–7]) is the production of exotic nuclides to the limit of the neutron dripline [8–10]. Nuclei situated far away from the line of beta stability offer a crucial insight into the astrophysical rapid neutron capture process (r-process) which plays a significant role in the production of half of the abundance of the nuclides heavier than iron [11,12]. In order to access these exotic nuclides with high neutron-excess, apart from the traditional approaches of projectile fragmentation, fission and spallation, it is necessary to pick up neutrons from the target [10]. Such multinucleon transfer mechanisms mainly take place in peripheral nucleon-exchange reactions at beam energies from the Coulomb barrier to the Fermi energy domain ( $\sim 15\text{--}20$  MeV/nucleon) [13,14]. For this reason, we initiated a project to produce and identify projectile-like fragments with the MAGNEX large-acceptance spectrometer at the INFN-LNS from the reaction of  $^{70}\text{Zn}$  (15 MeV/nucleon) +  $^{64}\text{Ni}$ . As presented in ref. [15], we have developed a systematic procedure to reconstruct the atomic number  $Z$  of the ejectiles along with their ionic charge states employing measurements of the energy loss,

\* Corresponding author: [stekoul@chem.uoa.gr](mailto:stekoul@chem.uoa.gr)

residual energy and time-of-flight. Subsequently, we moved on to obtain the momentum and angular distributions of the ejectiles and their production cross sections. Some of these experimental results alongside comparisons to theoretical models will be presented in this article. A more comprehensive presentation of our recent results is presented in [16].

## EXPERIMENTAL SETUP AND MEASUREMENTS

The experiment was carried out with the MAGNEX facility at the Istituto Nazionale di Fisica Nucleare, Laboratori Nazionali del Sud (INFN-LNS) in Catania, Italy. MAGNEX is a high-acceptance device which makes use of both the advantages of the traditional magnetic spectrometry and those of a large momentum and angular acceptance detector [17-19]. A beam of  $^{70}\text{Zn}^{15+}$  at 15 MeV/nucleon delivered by the K800 superconducting cyclotron bombarded a  $1.18 \text{ mg/cm}^2$   $^{64}\text{Ni}$  foil. The ejectiles emerging from the target passed through a  $6 \mu\text{m}$  Mylar stripper foil and then were momentum analyzed by the MAGNEX spectrometer and detected by its focal plane detector (FPD) [20,21].

The focal plane detector (FPD) is a large gas-filled hybrid detector with a wall of 60 large-area silicon detectors arranged in three rows at the end. It mainly consists of two parts: a gas tracker sensitive to the energy loss of the reaction products and a stopping wall of silicon detectors for the measurement of their residual energy. The detector mainly consists of a Mylar foil ( $6 \mu\text{m}$ ) at the entrance window and a proportional drift chamber spanning at six sequential planes, providing the energy loss and the coordinates of the ions. At the end of the detector, a wall of 60 silicon detectors is responsible for the extraction of the residual energy of each incident particle. Finally, the time-of-flight (TOF) of the ions was measured via a start signal from the silicon detectors of the FPD and a stop signal from the radiofrequency (RF) of the cyclotron. Further details of the experimental setup along with schematic diagrams are given in Ref. [17].

## PARTICLE IDENTIFICATION PROCEDURE

The particle identification procedure is based on a new technique that we developed in Ref. [15] and is influenced by the procedure presented in Ref. [21]. Our approach involves a reconstruction of the atomic number  $Z$  of the ejectiles using the measured and calibrated quantities of the total energy loss ( $\Delta E_{\text{cor}}$ ) in the gas section of the FPD (corrected for path length differences depending on the angle of incidence), the residual energy measured by the silicon detectors ( $E_{\text{resid}}$ ) and the TOF.

Subsequently, we employed a correlation of the reconstructed atomic number  $Z$  and the reconstructed ionic charge state  $q$  of the reaction products in a two-dimensional plot where we applied proper gating to select events of given  $Z$  and  $q$ . An example of this approach can be found in Ref. [15,16,22,23]. We then proceeded to the determination of the masses. This approach is mainly based on the relationship between the total kinetic energy of the ions and the magnetic rigidity expressed as:

$$B\rho = \frac{\sqrt{m}}{q} \sqrt{2 E_{\text{tot}}} \quad (1)$$

The above equation expresses a proportionality of the magnetic rigidity on  $\sqrt{E_{\text{tot}}}$  with a slope of  $\sqrt{m}/q$ . Thus, a correlation of  $B\rho$  on  $\sqrt{E_{\text{tot}}}$  or, (for simplicity) on  $E_{\text{tot}}$  should result on particle bands of the same  $\sqrt{m}/q$ . But since in our approach we have fixed  $q$ , the bands should correspond to successive masses.

The next step of our analysis was the extraction of momentum spectra, angular distributions and production cross sections. Having identified the isotopes (each characterized by  $Z$ ,  $q$  and  $A$ ) on each Si detector after setting proper graphical cuts in the  $B\rho$  versus  $E_{\text{tot}}$  plot, we have obtained a two-dimensional distribution of the reaction angle ( $\theta_{\text{lab}}$ ) versus magnetic rigidity ( $B\rho$ ). Each channel of this plot (events of a given  $\theta_{\text{lab}}$  and  $B\rho$  and their respective counts), is stored properly and used as input for

an appropriate data manipulation program developed in our lab. This program is responsible for constructing a four-dimensional distribution that yields the cross section with respect to  $Z$ ,  $A$ ,  $\theta_{\text{lab}}$  and momentum per nucleon ( $p/A$ ), leading to momentum distributions, as well as production cross sections of the ejectiles [16]. At this point, we need to comment that in our systematic analysis we have chosen to use the momentum per nucleon of the ions instead of the kinetic energy. The momentum per nucleon ( $p/A$ ) essentially expresses the velocity of the particles and is a measure of the energy dissipation caused by the interaction of the projectile-target binary system. Thus, providing important information on the mechanism responsible for the production of the fragments of interest. The general feature of the momentum distributions, as expected, is the presence of two main regions: a) a quasielastic peak that corresponds to direct processes, and b) a broad region, located at lower values of  $p/A$ , that corresponds to deep inelastic processes involving extensive multinucleon transfers.

## BRIEF OVERVIEW OF THEORETICAL MODELS

The calculations performed are based on a standard two-stage Monte Carlo approach. The dynamical stage of the interaction between the projectile and the target was described by two theoretical models: the phenomenological DIT model [24] and the microscopic CoMD model [25,26].

The DIT (Deep-Inelastic Transfer) model is a phenomenological model used for peripheral collisions in the Fermi energy domain. Initially, both the projectile and the target are assumed to be spherical, and they approach each other along Coulomb trajectories. When the di-nuclear system is within the range of nuclear interaction, it is represented as two Fermi gases in contact, which permits the stochastic exchange of nucleons through a “window” that opens between the touching nuclear surfaces.

The CoMD (Constrained Molecular Dynamics) model is a microscopic code that is based on the general approach of quantum molecular dynamics (QMD), describing the nucleons as localized Gaussian wavepackets that interact via an effective nucleon-nucleon interaction. The Pauli principle is imposed via a constraint in the phase space.

After the dynamical stage of the reaction, the de-excitation of the primary fragments was described by the statistical deexcitation GEMINI code [27].

## EXPERIMENTAL RESULTS AND COMPARISON WITH THEORETICAL CALCULATIONS

In this section, we present experimental results of ejectile distributions from the reaction of  $^{70}\text{Zn}$  (15 MeV/nucleon) with  $^{64}\text{Ni}$ , along with a comparison of the experimental data with theoretical calculations employing the aforementioned models.

We recall that the analysis of the data resulted in distributions with respect to  $Z$ ,  $A$ ,  $\theta_{\text{lab}}$  and  $p/A$ . To have a better understanding and a more thorough overview of the distributions of the reaction products, we have obtained two-dimensional distributions of  $p/A$  versus  $\theta_{\text{lab}}$  for various reaction channels. The y-axis represents  $p/A$  (MeV/c) and the x-axis represents the reaction angle (degrees). This type of correlations is commonly utilized in the study of deep-inelastic reactions near and above the Coulomb barrier providing information on the energy dissipation of the dinuclear complex [28]. In Fig. 1, we present plots of various channels of the reaction under study. In this figure, the horizontal dashed lines represent the projectile  $p/A = 164.4$  MeV/c, and the vertical dashed lines indicate the grazing angle  $\theta_{\text{gr}} = 6.5^\circ$  of the ejectiles of the reaction. The channels are denoted by the number of neutrons or protons added or removed from the projectile. A typical attribute in the majority of the channels shown is the presence of a peak (a “band”) near the velocity of the beam (quasielastic peak) and an extended region of lower velocities corresponding to more dissipative events.

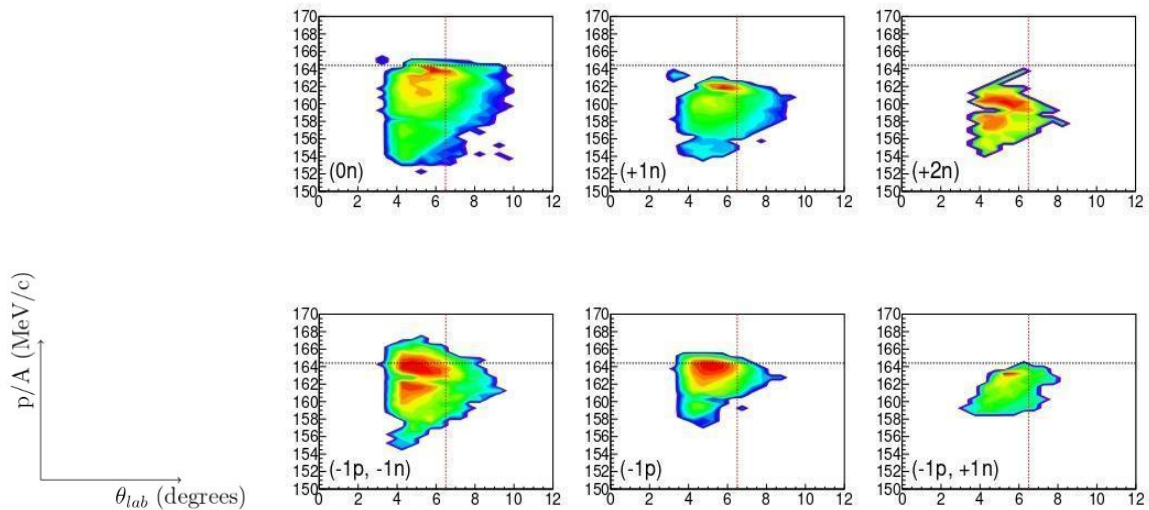


**Figure 1.**  $p/A$  versus  $\theta_{lab}$  distributions of ejectiles from representative channels of the reaction  $^{70}\text{Zn}$  (15 MeV/nucleon) +  $^{64}\text{Ni}$ . The horizontal dashed lines represent the  $p/A$  of the projectile and the vertical dashed lines the grazing angle. Channels are marked by the number of neutrons or protons added or removed from the projectile.

In Fig. 2 and 3, we present  $p/A$  distributions of neutron-rich ejectiles from the reaction of  $^{70}\text{Zn}$  (15 MeV/nucleon) +  $^{64}\text{Ni}$ , depicting the pickup of one neutron and two neutrons from the target (Fig. 2) and the removal of one and two protons (Fig. 3), respectively.

The vertical axis in the  $p/A$  distributions, denoted as “diff. cross section”, corresponds to  $d^2\sigma/d(p/A)d\Omega$  [mb/(MeV/c) msr]. The experimental data are shown by solid black circles. The DIT calculation is represented by open (blue) circles, while the CoMD calculation by open (red) squares. The green dashed line shown on each frame of the momentum distribution plot represents the momentum per nucleon of the beam, which is 164.4 MeV/c. The numbers reported in some peaks of the distributions are the total excitation energy of the quasiprojectile-quasitarget system, determined by the corresponding  $p/A$  values employing binary kinematics. We remind that the excitation energy is connected with the reaction  $Q$ -value through the following equation:

$$E_{tot} = Q_{gg} - Q_{ex}(2)$$

where  $Q_{gg}$  is the ground-state to ground-state  $Q$ -value of each channel, as shown on the right side of each  $p/A$  panel.

We observe in the  $p/A$  spectra shown in both Figures 2 and 3, that the DIT calculation is able to describe rather successfully the broad regions of the spectra in the depicted channels but cannot describe the quasielastic peak in some cases (e.g. the case of the one neutron pickup). This result is consistent with the fact that the DIT model has no inherent mechanism of inelastic excitation and direct transfer. For this reason, it cannot describe the quasielastic part of the experimental  $p/A$  spectrum. Regarding the CoMD/GEMINI calculation, we notice that it exhibits broad peaks at lower velocities than the data and tends to be higher than the data (e.g. in the case of one neutron pickup and one proton removal). It appears that the current set of parameters for the CoMD calculations tend to overestimate the yields of the proton removal channels. We are currently investigating this issue further.



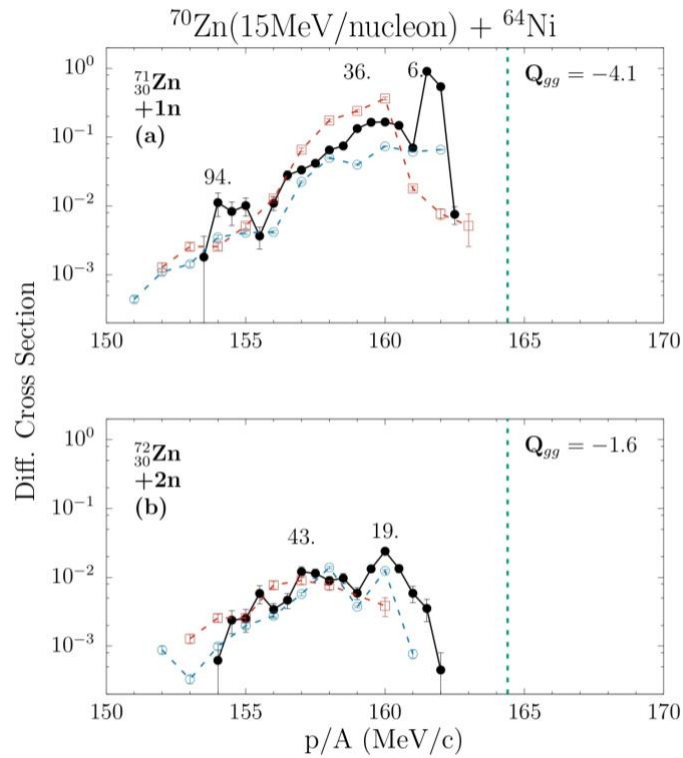


**Figure 2.** Momentum per nucleon distributions of ejectiles from neutron pickup channels from  $^{70}\text{Zn}$  (15 MeV/nucleon) +  $^{64}\text{Ni}$ . Experimental data: closed (black) circles. DIT calculation: open (blue) circles. CoMD calculation: open (red) squares. The vertical dashed (green) line is the  $p/A$  of the projectile.

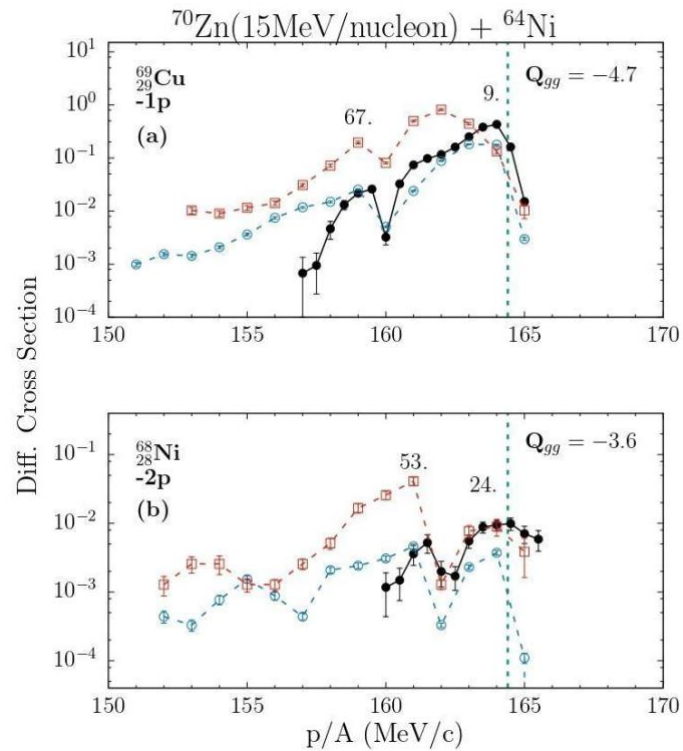


**Figure 3.** Momentum per nucleon distributions of ejectiles from proton removal channels from  $^{70}\text{Zn}$  (15 MeV/nucleon) +  $^{64}\text{Ni}$ . Experimental data: closed (black) circles. DIT calculation: open (blue) circles. CoMD calculation: open (red) squares. The vertical dashed (green) line is the  $p/A$  of the projectile.

## CONCLUSIONS

In this work, we presented some of our experimental results of the various distributions of ejectiles from the reaction of a  $^{70}\text{Zn}$  beam at 15 MeV/nucleon energy with a  $^{64}\text{Ni}$  target that was carried out with the use of the MAGNEX spectrometer. This is our first systematic effort to study peripheral reactions with medium mass-heavy ions by employing a large acceptance spectrometer to obtain momentum distributions, as well as production cross sections and angular distributions.

The experimental data were compared with two dynamical models, the DIT and the CoMD, followed by the de-excitation code GEMINI. The DIT model offered an overall fair description of the processes involving nucleon exchange, but could not describe the quasielastic part in some of the channels. The CoMD model gave an overall, but less accurate description of the data, indicating that further developments are needed, which are currently underway.

This work constitutes one of the very few high-resolution mass-spectrometric studies in this energy domain. We expect that the thorough examination of the present data, along with detailed theoretical calculations and cross-comparisons with previous works of our research group [29-31], will lead to a better understanding of the reaction mechanisms that dominate this energy regime.

## References

- [1] FRIB main page: [www.frib.msu.edu](http://www.frib.msu.edu)
- [2] GANIL main page: [www.ganil.fr](http://www.ganil.fr)
- [3] GSI main page: [www.gsi.de](http://www.gsi.de)
- [4] RIBF: [www.nishina.riken.jp/facility/RIBFabout\\_e.html](http://www.nishina.riken.jp/facility/RIBFabout_e.html)
- [5] ATLAS: [www.phy.anl.gov/atlas/facility/index.html](http://www.phy.anl.gov/atlas/facility/index.html)
- [6] INFN/LNS main page: [www.lns.infn.it](http://www.lns.infn.it)
- [7] RISP main page: [www.risp.re.kr/eng/pMainPage.do](http://www.risp.re.kr/eng/pMainPage.do)
- [8] G.G. Adamian et al., Eur. Phys. J. A 56, 47 (2020); doi: 10.1140/epja/s10050-020-00046-7
- [9] T. Mijatovic, Front. Phys. 10, 965198 (2022); doi: 10.3389/fphy.2022.965198
- [10] Y.X. Watanabe et al., Phys. Rev. Lett. 115, 172503 (2015); doi: 10.1103/PhysRevLett.115.172503
- [11] H. Grawe et al., Rep. Prog. Phys. 70, 1525 (2007); doi: 10.1088/0034-4885/70/9/R02
- [12] A. Arcones and F.K. Thielemann, Astron. Astrophys. Rev. 31, 1 (2023); doi: 0.1007/s00159-022-00146-x
- [13] T. Mijatovic et al., Phys. Rev. C 94, 064616 (2016); doi: 10.1103/PhysRevC.94.064616
- [14] L. Corradi et al., J. Phys. G 36, 113101 (2009); doi: 10.1088/0954-3899/36/11/113101
- [15] G.A. Souliotis et al., NIM A 1031, 166588 (2022); doi: 10.1016/j.nima.2022.166588
- [16] S. Koulouris et al., Phys. Rev. C 108, 044612 (2023); doi: 10.1103/PhysRevC.108.044612
- [17] F. Cappuzzello et al., Eur. Phys. J. A 52, 167 (2016); doi: 10.1140/epja/i2016-16167-1
- [18] F. Cappuzzello et al., NIM A 621, 419 (2010); doi: 10.1016/j.nima.2010.05.027
- [19] A. Cunsolo et al., NIM A 481, 48 (2002); doi: 10.1016/S0168-9002(01)01357-2
- [20] M. Cavallaro et al., Eur. Phys. J. A 48, 59 (2012); doi: 10.1140/epja/i2012-12059-8
- [21] D. Torresi et al., Nucl. Instr. and Meth. A 989, 164918 (2021); doi: 10.1016/j.nima.2020.164918
- [22] S. Koulouris et al., EPJ Web of Conf. 252, 07005 (2021); doi: 10.1051/epjconf/202125207005
- [23] S. Koulouris et al., HNPS Adv. Nucl. Phys. 28, 42 (2022); doi: 10.12681/hnps.3571
- [24] L. Tassan-Got and C. Stephan, Nucl. Phys. A 524, 121 (1991); doi: 10.1016/0375-9474(91)90019-3
- [25] M. Papa, T. Maruyama, A. Bonasera, Phys. Rev. C 64, 024612 (2001); doi: 10.1103/PhysRevC.64.024612
- [26] M. Papa et al., J. Comp. Phys. 208, 403 (2005); doi: 10.1016/j.jcp.2005.02.032
- [27] R. Charity et al., Nucl. Phys. A 483, 371 (1988); doi: 10.1016/0375-9474(88)90542-8
- [28] V. Zagrebaev, W. Greiner, J. Phys. G 31, 825 (2005); doi: 10.1088/0954-3899/31/7/024
- [29] A. Papageorgiou et al., J. Phys. G 45, 095105 (2018); doi: 10.1088/1361-6471/aad7df
- [30] O. Fasoula et al., HNPS Adv. Nucl. Phys. 28, 47 (2022); doi: 10.12681/hnpsanp.5089
- [31] K. Palli et al., EPJ Web of Conf. 252, 07002 (2021); doi: 10.1051/epjconf/202125207002